**Journal of the Earth & Space Physics. Vol. 33, No. 1, 2007, P. 1-12**

# Perturbations in orbital elements of a low earth orbiting satellite

Eshagh, M[1*]. and Najafi Alamdari, M[2].

[1]*Ph.D student of Geodesy, Royal Institute of Technology, Stockholm, Sweden*
[2]*Assistant Professor, Geodesy Department, Khajeh Nasir Toosi University of Technology, Tehran, Iran*

*(Received: 8 Jun 2005, Accepted: 7 Feb 2007)*

**Abstract**

The main point of this paper is to evaluate the perturbations in orbital elements of a low Earth orbiting satellite. The outcome of a numerical orbit integration process is the position and velocity vectors of satellite in an inertial coordinate system. The velocity and position vectors are converted into the corresponding orbital elements. Perturbations in a satellite motion affect the orbital elements in the sense of Keplerian motion. In this paper after introducing the perturbing forces acting on a satellite, the method of converting the position and velocity into the orbital elements is presented, and finally the perturbations in orbital elements of the low Earth orbiting satellite of CHAMP are evaluated. The numerical results show that, disregarding the geopotential perturbing forces, the air drag is the most predominant among other perturbing forces: rotational deformation, solar radiation, third body effect, solid Earth tide, ocean tide, and general relativity arranged by their magnitude respectively.

**Key words:** Orbit, Perturbations, CHAMP, Orbital elements, Gravitation, Air drag

## 1 INTRODUCTION

The geodetic satellites have two major missions, a satellite can be either used for positioning in geodesy or it can be employed as a sensor for measuring the external gravity field of the Earth. A majority of the positioning satellites are medium orbiting with altitude above 1000 km. Most of the satellites at 1000 km altitude are launched with the aim of remote sensing and imaging. The low Earth orbiting satellites (1000 km or lower) are suitable for recovering the gravity field of the Earth. Because of their low altitudes, the perturbations in orbits are larger than the perturbations in higher orbits. Hence, they are detectable in orbit analysis for the gravity field determination. According to Kepler's first law the satellite's trajectory will be an ellipse, which the Earth is focused on, if the Earth gravity field resembles a central field. In the first approximation, the gravity field is central. Then the major force keeping the satellite in its orbit is the central gravitational force part due to the spherical Earth which drives the satellite into the Keplerian orbit. The remaining forces, i.e., the pertubing forces are driving the satellite out of the Keplerian orbit. Such forces are classified into two major groups as gravitational and non-gravitational perturbing force, c.f., Eanes and Bettapur (1995), Seeber (2003), Hofmann et al (2001), Eshagh et al (2003), Eshagh (2003a), and Leick (1995). It can be seen that the gravitational perturbing forces due to the Earth have greater effects, hence larger and sensible due perturbations on closer satellites. The perturbation is defined to be the separation between a satellite's real orbit and the average Keplerian orbit, best fitting the real orbit. Precise evaluation of a perturbation requires the precise evaluation of the real orbit at first. CHAMP is a satellite orbiting 500 km above the Earth at the moment. The perturbations are profound and measurable for the precise determination of the gravity field. Wolf (2000) has worked on some low Earth orbiting satellites of about 1000 km altitude, Su (2000) studied the GEO, MEO satellites and like GPS, GLONAS, Santos (1994) investigated the real time kinematics orbit improvements of GPS satellites for short and long baseline computations, Eanes et al. (1995) worked on geodynamics satellites, and Buffet (1985) studied the perturbations of orbital elements of the GPS satellites. All of these researchers have worked on the satellites of altitude larger than 800 km. In this research, the CHAMP satellite is considered for the investigation. Some of the gravitational and non-gravitational perturbing forces which are not effective in higher altitude, come in effect at the altitude of CHAMP. Eshagh and Najafi Alamdari (2003, 2005a, 2005b, and 2005c) have studied the numerical integration methods, orbital perturbations of low Earth orbiting satellites. They compared different numerical integration methods and forces acting on a low orbiting

[*]Corresponding author: Tel: +46 8 7907369 Fax: +46 8 7907343 E-Mail: eshagh@kth.se

satellite. They have also studied the CHAMP satellite orbit as a case study. Eshagh (2003a) continued studying the perturbations in the directions of radial, along track, and across track of a low orbiting satellite due to the gravitational and non-gravitational and non-central forces acting up on. Eshagh (2003b) investigated the numerical integrations in orbit determination and due errors in conjunction with the maximum degree and order of geopotential coefficients responsible for the perturbations. It was found that a geopotential model complete up to the degree and order of 30 suffices for the orbit integration using Runge-Kutta of the 4-th order. Also Eshagh (2005c) suggested a step variable method for the orbit integration.

In the second section of this paper the perturbing forces are introduced after the method of integration is selected. Next, the method of converting position and velocity of a satellite into orbital elements are presented and finally the perturbations of orbital elements of a low Earth orbiting satellite are computed.

## 2 PERTURBING FORCES ACTING ON A SATELLITE

The equation of motion of a satellite is influenced by all the forces in action. The equation of motion of a near Earth satellite is described in an internal reference system of coordinates in the form of differential equations of accelerations. By integrating the perturbing accelerations, the position and velocity of the satellite at an instant of time is computed. The accelerations are divided into two major groups: gravitational and non-gravitational.

### 2-1 GRAVITATIONAL ACCELERATIONS

The gravitational accelerations consist of geopotential perturbing acceleration, solid Earth tide effect, ocean tide effect, rotational deformation of the Earth, third body effects, and relativistic effect especially general relativity for a low Earth orbiting satellite.

#### 2-1-1 GEOPOTENTIAL PERTURBATION

The gravitational potential due to the Earth can be expressed in terms of a series of spherical harmonic functions. In a body fixed reference coordinates system, $U_{geo}$ is modeled as in Rim and Schutz (2001).

$$U_{geo}(r,\theta,\lambda) = \frac{GM_e}{r} + \frac{GM_e}{r}\sum_{l=1}^{\infty}\sum_{m=0}^{l}\left(\frac{a_e}{r}\right)^l \overline{P}_{lm}(\sin\theta)\left[\overline{C}_{lm}\mathrm{Cos}m\lambda + \overline{S}_{lm}\mathrm{Sin}m\lambda\right] \quad (1)$$

where, $GM_e$ is the gravitational constant multiplied by the mass of the Earth, $a_e$ is the mean equatorial radius of the Earth, $\overline{C}_{lm}, \overline{S}_{lm}$ are the normalized spherical harmonic coefficients, $\overline{P}_{lm}(\mathrm{Sin}\ )$ is the normalized associated Legendre function, $r,\theta,\lambda$ are the spherical coordinates of a computation point.

#### 2-1-2 SOLID EARTH TIDE

The temporal potential variations $\Delta U_{st}$ due to the solid tide can also be expressed in terms of the spherical harmonics with coefficients $\Delta\overline{C}_{nm}$ and $\Delta\overline{S}_{nm}$ as the temporal corrections to geopotential coefficients $\overline{C}_{nm}$ and $\overline{S}_{nm}$. They are expressed in terms of the tidal amplitude coefficients $H_k$ as in Rim and Schutz (2001), Wolf (2000):

$$\Delta\overline{C}_{lm} = \frac{(-1)^m}{a_e\sqrt{4\pi(2-\delta_{0m})}}\sum_k K_k^0 H_k \begin{cases}\mathrm{Cos}\theta_k\\ \mathrm{Sin}\theta_k\end{cases} \quad (2)$$

where for l-m even, the cosine term is used and for l-m odd, the sine term is used

$$\Delta\overline{S}_{lm} = \frac{(-1)^m}{a_e\sqrt{4\pi(2-\delta_{0m})}}\sum_k K_k^0 H_k \begin{cases}-\mathrm{Sin}\theta_k\\ \mathrm{Cos}\theta_k\end{cases} \quad (3)$$

where unlike the previous order, for l-m even the sine term is used and for l-m odd, the cosine term is used (Rim and Schutz, 2001). $\delta_{0m}$ is the Kroneker delta. The second love number $K_2$ is not a constant function. According to Wahr model it depends on the frequency of solid tide.

#### 2-1-3 OCEAN TIDE

The ocean tide and its loading deformation potential $\Delta U_{ot}$ as a perturbation due to the luni-solar gravity field can also be expressed in terms of spherical harmonics, i.e., temporal variations in the geopotential coefficients (Rim and Schutz, 2001 and Wolf 2000):

$$\Delta\overline{C}_{lm} = F_{lm}\sum_k A_{klm}, \Delta\overline{S}_{lm} = F_{lm}\sum_k B_{klm}, \quad (4)$$

where $F_{lm}, A_{klm}, B_{klm}$ are given as

$$F_{lm} = \frac{4\pi a_e{}^2 P_w}{M_e}\sqrt{\frac{(l+m)!}{(1-m)!(2l+1)(2-Sum)}}\left(\frac{1+k'_l}{2l+1}\right) \tag{5}$$

and

$$\begin{bmatrix} A_{klm} \\ B_{klm} \end{bmatrix} = \begin{bmatrix} \left(C^+_{klm} + C^-_{klm}\right) \\ \left(S^+_{klm} - S^-_{klm}\right) \end{bmatrix} Cos\theta_K + \begin{bmatrix} \left(S^+_{klm} + S^-_{klm}\right) \\ \left(C^-_{klm} - C^+_{klm}\right) \end{bmatrix} Sin\theta_k \tag{6}$$

where the required parameters are also given in a Global Ocean Tides Model.

## 2-1-4 ROTATIONAL DEFORMATION

Any changes in the angular velocity vector $\vec{\omega}$ of the Earth will be producing a variable centrifugal force field resulting a deformation and as such a perturbation would occur in the Earth centrifugal potential. The variation of potential due to this effect can be written as in Rim and Schutz (2001):

$$\Delta C_{20} = \frac{a_e^3}{6GM_e}\left(m_1^2 + m_2^2 - 2(1+m_3)^2\right)\Omega^2 K_2 \approx \frac{-a_e^3}{3GM_e}(1+2m_3)\Omega^2 K_2 \tag{7}$$

$$\Delta C_{21} = \frac{-a_e^3}{3GM_e} m_1(1+m_3)\Omega^2 K_2 \approx \frac{-a_e^3}{3GM_e} m_1 \Omega^2 K_2 \tag{8}$$

$$\Delta S_{21} = \frac{-a_e^3}{3GM_e}(m_2(1+m_3))\Omega^2 K_2 \approx \frac{-a_e^3}{3GM_e} m_2 \Omega^2 K_2 \tag{9}$$

$$\Delta C_{22} = \frac{a_e^3}{12GM_e}\left(m_2^2 - m_1^2\right)\Omega^2 K_2 \approx 0 \tag{10}$$

$$\Delta S_{22} = \frac{-a_e^3}{6GM_e}(m_2 m_1)\Omega^2 K_2 \approx 0\ , \tag{11}$$

$m_1 = x_p$, $m_2 = -y_p$ , $m_3 = \frac{d(UT\,1 - IAT)}{d(IAT)}\Omega$ is the mean angular velocity of the Earth, $m_i$ are small unit less quantities related to the polar motion and the Earth rotation.

## 2-1-5 THIRD BODY EFFECT

This perturbing gravitation implied by a third body, e.g., the Moon or the Sun, is easily describable in a geocentric Cartesian coordinates system. It is the gravitational acceleration exerted on the satellite by the third body minus the acceleration exerted on the Earth by the same body (Rim and Schutz, 2001, Buffet, 1985 and Seeber, 2003):

$$\vec{a}_{tb} = \sum_i GM_i\left[\frac{\vec{r}_i}{\left\|r_i^3\right\|} - \frac{\vec{\Delta}_i}{\left\|\Delta_i^3\right\|}\right] \tag{12}$$

where, $r_i$ is the position vector of the third body number i, $M_i$ is the mass of third body, $\Delta_i$ is the position vector of third body from the satellite. This equation is written in an inertial coordinate system.

## 2-1-6 GENERAL RELATIVITY

The general relativity perturbation on the near Earth satellite can be modeled as in McCarthy (1990) and Santos (1994):

$$\vec{a}_{rel} = \frac{GM_e}{C^2 r^3}\left\{(2\beta + 2\gamma)\frac{GM_e}{r} - \gamma\gamma\left(\vec{r}.\vec{r}\right) + (2+2\gamma)\left(\vec{r}.\dot{\vec{r}}\right)\dot{\vec{r}}\right\} \tag{13}$$

where, C is the speed of light in the geocentric frame, $\vec{r}, \dot{\vec{r}}$ are the geocentric satellite position and velocity vectors, $GM_e$ is the gravitational constant for the Earth and $\beta, \gamma$ are the parameterized post-Newtonian (PPN) parameters.

## 2-2 NON-GRAVITATIONAL ACCELERATIONS

Among the non-gravitational forces, the atmospheric drag and solar radiation pressure will be considered as follows:

### 2-2-1 ATMOSPHERIC ACCELE RATION

When a satellite is orbiting around the Earth, it collides with the Earth's atmosphere. Hence a friction between the satellite and the atmosphere is produced. As a result a deceleration of satellite occurs. It is proportional to the satellite velocity and density of the atmosphere. When the velocity is increased, the acceleration is increased too. Since the atmospheric density at low altitude is increased, the acceleration of the satellite when passing on the perigee is increased. In the apogee, the deceleration is reduced. As a result, the satellite trajectory becomes more circular. This effect of course, depends on the

shape and orientation of the satellite. Anear Earth satellite of an arbitrary shape moving with a velocity of $\vec{v}$ in an atmosphere of density $\rho$ will experience drag forces. The drag acceleration is formulated as in Rim and Schutz, (2001) and Seeber (2003)

$$\vec{a}_{drag} = -\frac{1}{2}\rho\left(C_d \frac{A}{m}\right)\left|\vec{V}_r\right|\vec{V}, \qquad (14)$$

where, $\vec{V}_r$ is the satellite velocity relative to the atmosphere, m is the mass of satellite, $C_d$ is the drag coefficient specific to the satellite and A is the cross-sectional area of the main body perpendicular to $\vec{V}_r$.

### 2-2-2 SOLAR RADIATION PRESSURE

The solar radiation pressure or force is towards the satellite from the Sun. It is inversely proportional to the mass of the satellite. If the satellite is light and large then it is more affected. If the satellite is heavy and small it is less affected by the solar radiation. The satellite is constructed of materials that carry different refectories therefore modulation of such perturbation is very complicated. The sun radiates a constant amount of photons per unit of time. The radiation pressure is characterized as a momentum flux having an average value of $4.56\times10^{-6}\,N/m^2$ (Rim and Schutz, 2001), The direct solar radiation pressure from the sun on a satellite is modeled as in Rim and Schutz (2001):

$$\vec{a}_{solar} = -p(1+\eta)\frac{A}{m}\nu\,\hat{u} \qquad (15)$$

where, P is the momentum flux due to the sun, $\eta$ is the reflectivity coefficient of the satellite, A is the cross-sectional area of the satellite normal to the sun, m is the mass of the satellite, $\nu$ is the eclipse factor ($\nu = 0$ if the satellite is in full shadow , $\nu = 1$ if the satellite is in full sun, and $0 < \nu < 1$ if the satellite is in partial shadow.) and $\hat{u}$ is the unit vector pointing from satellite to the sun. The reflectivity coefficient $\eta$ represents the average value over the whole satellite rather than the virtual surface reflectivity in the conical or cylindrical shadow models for the Earth.

## 3 POSITION AND VELOCITY TO ORBITAL ELEMENTS CONVERSIONS

The integrated position and velocity of the satellites in the inertial space is converted to the orbital elements. The orbit period T reads as

$$T = 2\pi\sqrt{\frac{a^3}{GM}} \qquad (16)$$

where a is the major semi-axis of the orbit. There are three fundamental vectors $\vec{e}, \vec{h}$, and $\vec{n}$, Seeber (2003), shown in Figure 1, characterizing the motion of the satellite,

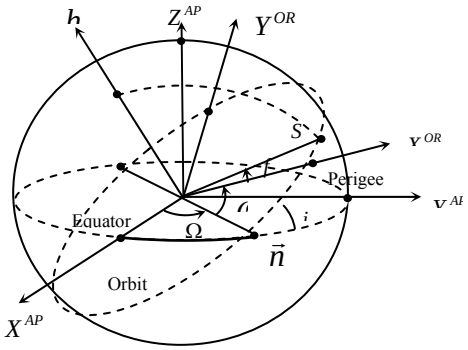


**Figure 1.** Fundamental vectors, (Eshagh and Najafi Alamdari, 2003).

where $\vec{h}$ the angular momentum of satellite and $\vec{n}$ in the direction of the ascending node given as

$$\vec{h} = \vec{r}\times\vec{v}, \qquad (17)$$

$$\vec{n} = \vec{h}\times\vec{z}, \qquad (18)$$

where $\vec{Z}$ is the unit vector along Z-axis of the inertial XYZ-system, the perigee vector $\vec{e}$ is given in Seeber (2003) as

$$\vec{e} = \frac{1}{GM}\left(\left(\left\|\vec{v}^2\right\| + \frac{GM}{\|\vec{r}\|}\right)\vec{r} + (\vec{r}.\vec{v})\vec{v}\right) \qquad (19)$$

with the three vectors $\vec{h}, \vec{n}, \vec{e}$ given above, the orbital elements are derived as in Seeber (2003):

$$\cos i = \frac{\vec{h}.\vec{z}}{h}, \quad \cos\Omega = \frac{\vec{n}.\vec{x}}{n} \qquad (20)$$

$$\cos\omega = \frac{\vec{n}.\vec{e}}{n.e}, \quad \cos f = \frac{\vec{e}.\vec{r}}{er} \qquad (21)$$

where f the true anomaly is related to the mean anomaly $\overline{M}$ through

$$\cos E = \frac{e + \cos f}{1 + e\cos f}, \tag{22}$$

$$\overline{M} = E - e\sin E, \tag{23}$$

Seeber (2003), Hofmann et al. (2001), and the semi major axis is computed by the following relation

$$a = \frac{p}{1 - e^2}, \tag{24}$$

$$p = \frac{h^2}{GM} \tag{25}$$

For an inclination between 0 and 90 a satellite motion is towards the east and it is called a direct motion. For an inclination between 90 and 180 the motion is oriented westward and it is called a retrograde motion.

## 4 NUMERICAL INTEGRATION

The second order differential equations of motion in the Earth's central gravity field are

$$\ddot{\vec{r}} = -\frac{GM}{r^3}\vec{r} + k \Rightarrow \begin{cases} \ddot{\vec{x}} = -\frac{GM}{r^3}\vec{x} = \begin{cases} \dot{x} = v_x \\ \dot{v}_x = -\frac{GM}{r^3}x + k_x \end{cases} \\ \ddot{\vec{y}} = -\frac{GM}{r^3}\vec{y} = \begin{cases} \dot{y} = v_y \\ \dot{v}_y = -\frac{GM}{r^3}y + k_y \end{cases} \\ \ddot{\vec{z}} = -\frac{GM}{r^3}\vec{z} = \begin{cases} \dot{z} = v_z \\ \dot{v}_z = -\frac{GM}{r^3}z + k_z \end{cases} \end{cases}$$

$$= \begin{cases} \dot{x} = v_x = f_1(x, y, z, \dot{x}, \dot{y}, \dot{z}) \\ \dot{y} = v_y = f_2(x, y, z, \dot{x}, \dot{y}, \dot{z}) \\ \dot{z} = v_z = f_3(x, y, z, \dot{x}, \dot{y}, \dot{z}) \\ \dot{v}_x = -\frac{GM}{r^3}x = f_4(x, y, z, \dot{x}, \dot{y}, \dot{z}) \\ \dot{v}_y = -\frac{GM}{r^3}y = f_5(x, y, z, \dot{x}, \dot{y}, \dot{z}) \\ \dot{v}_z = -\frac{GM}{r^3}z = f_6(x, y, z, \dot{x}, \dot{y}, \dot{z}). \end{cases} \tag{26}$$

Eshagh and Najafi Alamdari (2003).

Equation (26) is the system of differential equations of motion of a satellite in the central field. For the real field, the perturbing accelerations are added into the last three equations. For more details refer to the Eshagh and Najafi Alamdari (2003).

## 5 NUMERICAL RESULTS

One essential mission of a geodetic satellite is to determine the gravity field of the Earth. Such satellite usually have near polar orbit with very low and close to the Earth's surface in order to detect and sense the gravity field features better. The German geo-scientific satellite CHAMP (Challenging Mini satellite Payload) was launched in summer 2000 into an almost circular near polar orbit. Its altitude is about 454 Km. and inclination of 87.3 Deg. The period of one revolution of this satellite around the Earth is about 16 minutes. This satellite has the following advantages. The satellite is continuously tracked by maximum 12 GPS satellites simultaneously. CHAMP experiences an enhanced gravitational signal because of the low altitude. The direct on-orbit measurements of the non-gravitational satellite accelerations replace the insufficient models of air density and radiation pressure. The precise orbit of CHAMP is determined by combining the numerical integration method and GPS observations, namely the high-low technique of satellite-to-satellite tracking is used.

According to Figure 2, the perturbation in the semi major axis of the orbital ellipse has a periodic behavior. It changes about 20000 m during one revolution. Also, the inclination of the orbit changes of about 14 seconds and twice in one revolution. The right ascension of ascending node has a secular behavior as well as a periodic change with low amplitude. It changes about 1.5 minute during one revolution. Perigee argument has a periodic variation as well as a simple secular. Variations up to 10 degree can be seen in this element. Eccentricity has a complex behavior it seems to have two types of periodic variations. Its maximum change is about 0.0004. Mean anomaly of the satellite has periodic variations and it changes maximum 15 degree in one revolution. Comparing GPS satellite and computations according to Buffet (1985) one can see that the semi major axis of GPS satellites is changing about 2000 m in one revolution. The same behaviors of orbital elements of GPS satellites and CHAMP satellite can be seen but the magnitude of variations differ from each other.

Figure 3 shows the perturbations due to the solid Earth tide. The semi major axis of satellite has a periodic behavior and it changes about 1

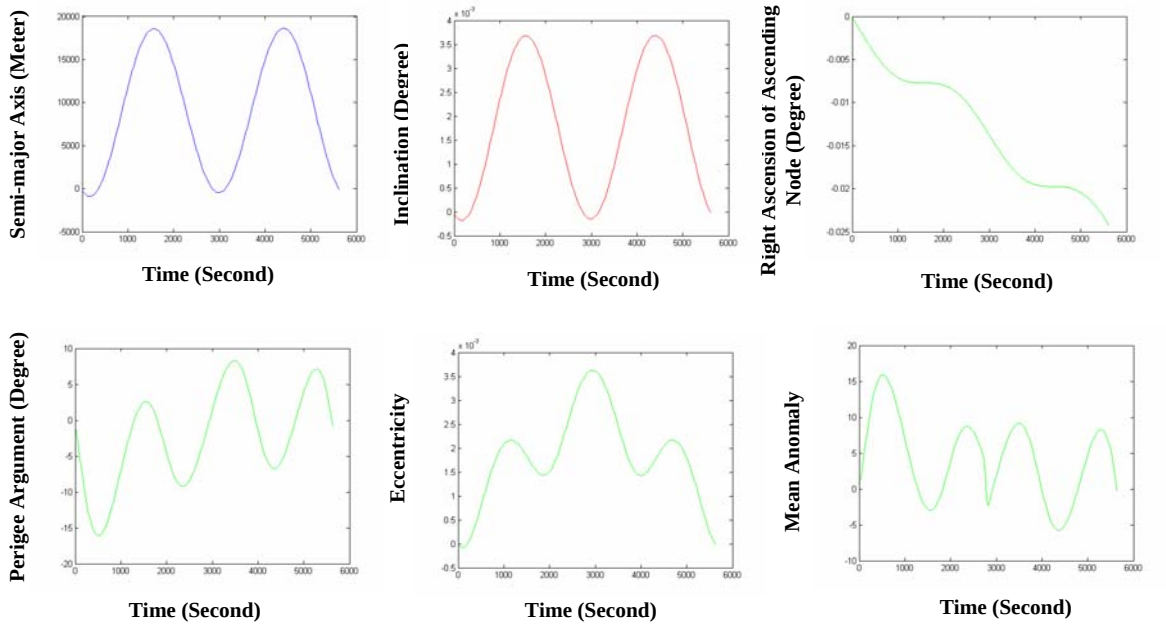


**Figure 2.** The Behavior of Keplerian Element due to the geopotential perturbation up to degree and order 30.

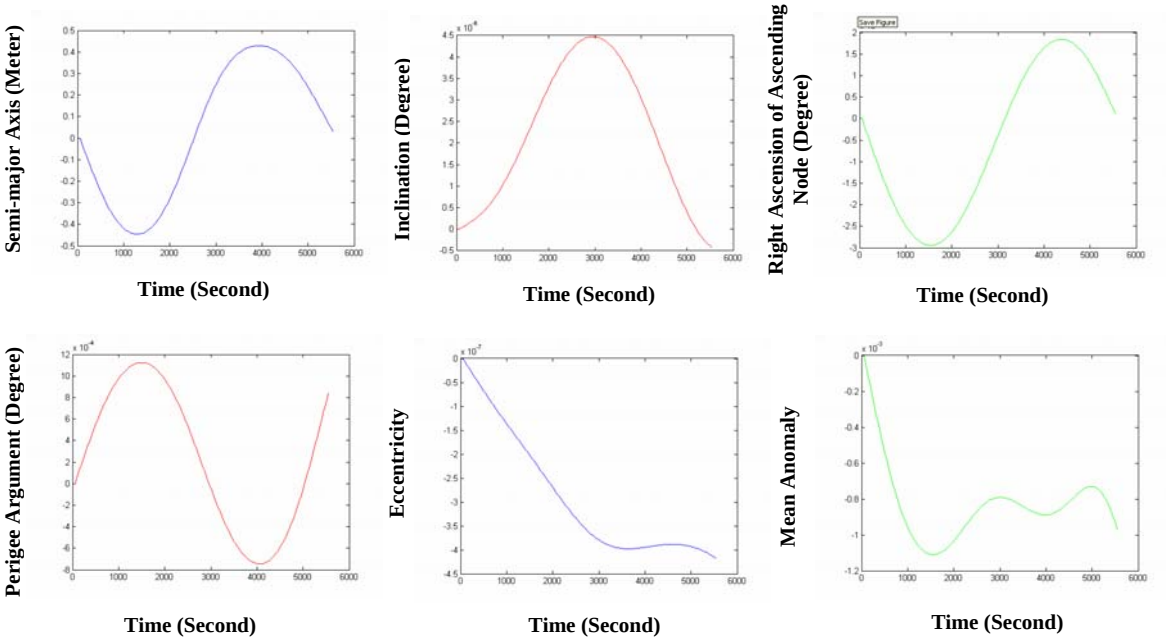


**Figure 3.** Perturbation due to the solid earth tide in orbital elements in 1 revolution.

meter in one revolution. The solid Earth tide changes the inclination of the orbit about at about $4.5\times10^{-4}$ equivalent to about 2 seconds in one revolution. The right ascension of the ascending node has also periodic variations. It changes about 3 degrees in one revolution of the satellite. The argument of perigee changes faster. Eccentricity seems to have secular variations. The mean anomaly has complex behavior and it is not easily interpreted, but its variations reach 10 seconds. It should be mentioned that the solid Earth tide does not much affect the medium height and geostationary satellites.

Figure 4 shows the third body effect on orbit of low Earth satellites. The variations of the semi major axis are periodic and the maximum variation is about 0.7 meter in one revolution, the inclination has the secular behavior. The right ascension of ascending node behavior is periodic. The perigee argument has also periodic behavior and maximum change of about tow seconds can be seen in one revolution. The eccentricity seems to have also periodic variation. The mean anomaly has complex behavior. It seems to have secular and periodic variations as well.

Figure 5 shows the general relativity effect in the orbit of low Earth orbiting satellite. The perturbations are though small. The results may be contaminated by the integration errors. The maximum variation is about 0.08 m in the semi major axis, the right ascension of ascending node, mean anomaly, and eccentricity elements seem to have periodic variations. Perigee argument has complex behavior of secular and periodic variation, but interpretation of behavior of the semi major and inclination is complicated.

Figure 6 shows the ocean tide effects on the orbit. The effects on the orbital elements are very small as in the case of general relativity. As can be seen the semi major axis of the satellite varies about 0.2 meter in periodic fashion.

Figure 7 shows the effects of the rotational deformation of the Earth. The effect on the semi major axis of the orbital ellipse is about 3 m in one revolution. As one can see, most of the orbital element behavior is more or less periodic except the right ascension of the ascending node which has secular variation. Now let us now consider two main non-gravitational forces, namely the solar radiation pressure and the air drag. Of course it should be mentioned that the thermal effect and the Earth radiation pressure are classified as non-gravitational forces but their computations are very complicated.

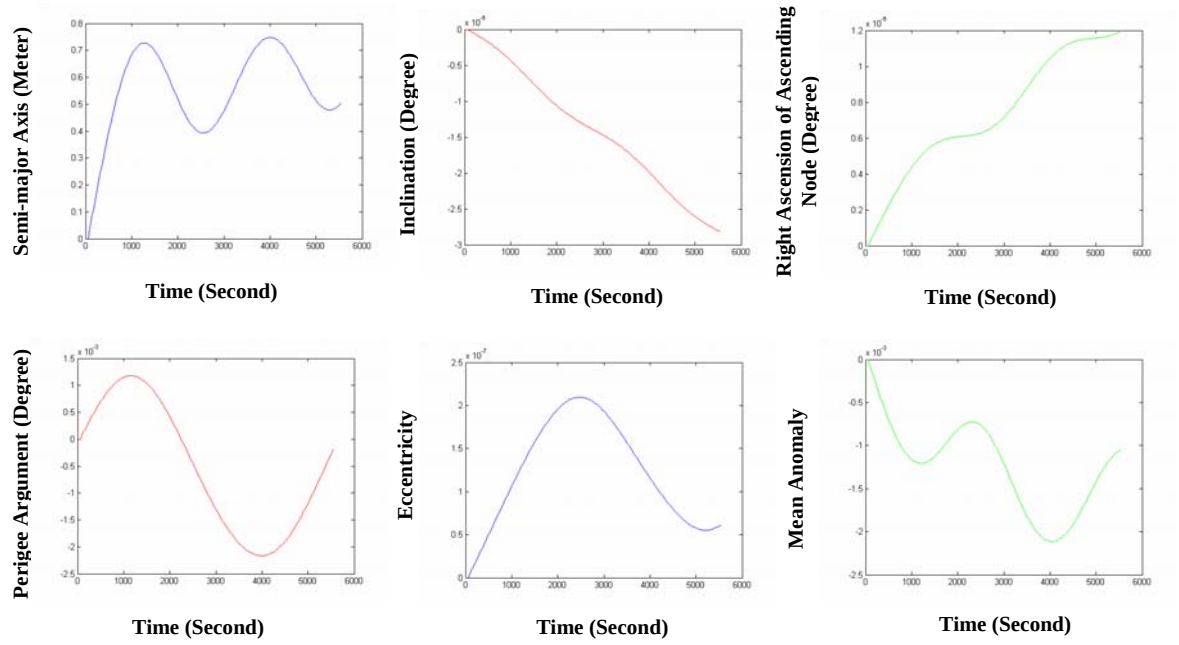


**Figure 4.** The perturbation due to the third bodies in orbital elements in 1 revolution.

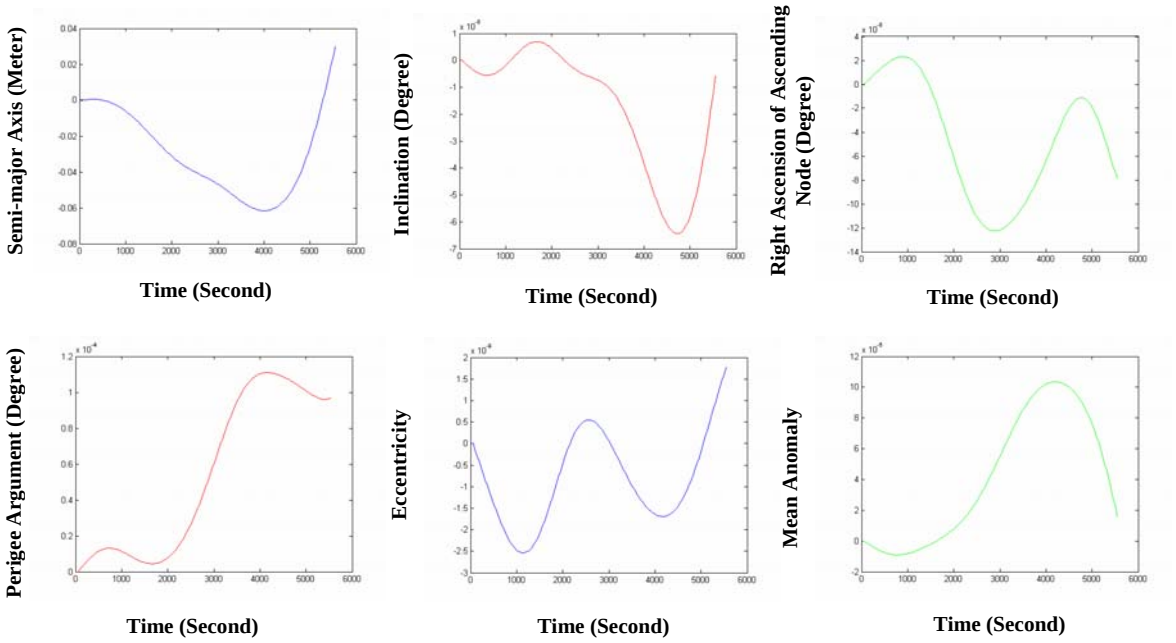


**Figure 5.** The perturbation due to the general relativity in orbital elements in 1 revolution.

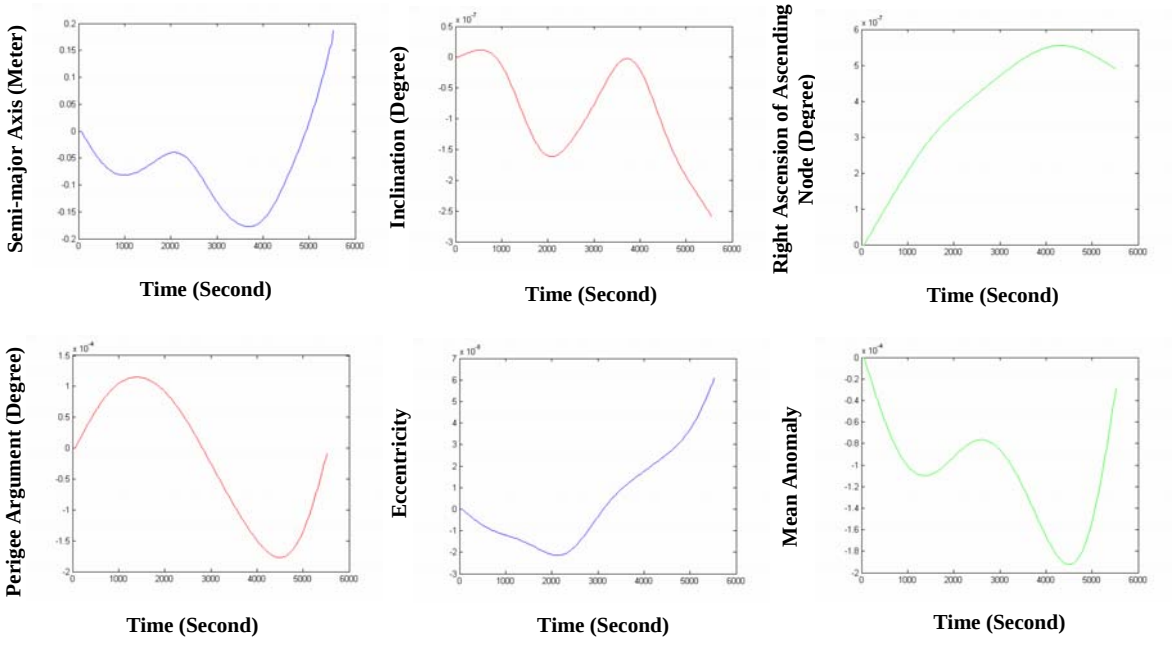


**Figure 6.** The perturbation due to the ocean tide in orbital elements in 1 revolution.

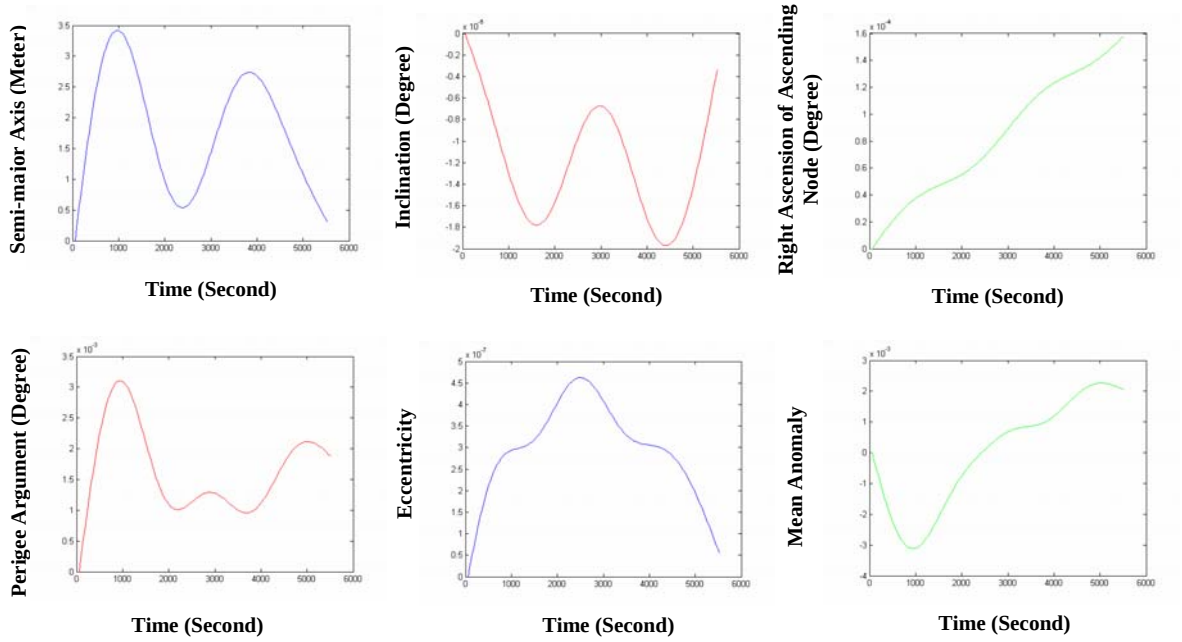


**Figure 7.** The perturbation due to the rotational deformation in orbital elements in 1 revolution.

Figure 8 shows the variations on the elements due to the solar radiation pressure. The semi major axis of the orbital ellipse, inclination, right ascension of ascending node, and the mean anomaly of the satellites have periodic behavior whereas the perigee and eccentricity variations are secular.

Air drag is reducing the size of the semi major of orbital ellipse continually. As seen in figure 9, it is secularly reduced by 6 m in one revolution. Perigee argument, eccentricity, and mean anomaly have periodic treatment, and inclination and right ascension of ascending node treats as secular. The summary of the above numerical results are presented in table 1.

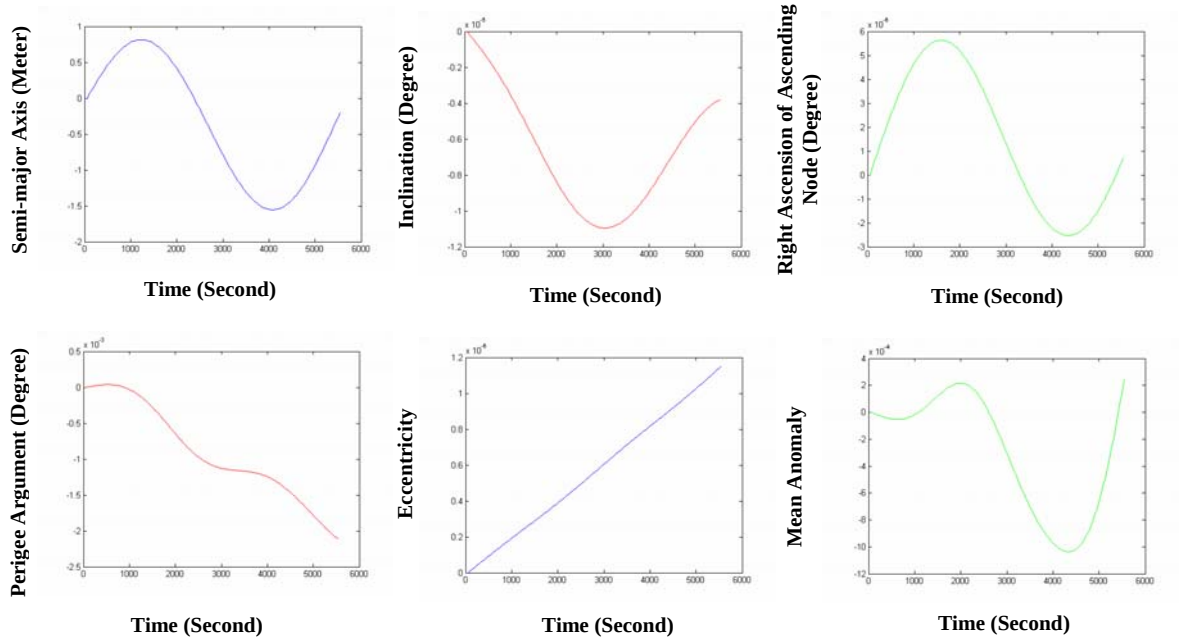


**Figure 8.** The perturbation due to the solar radiation pressure in orbital elements in 1 revolution.

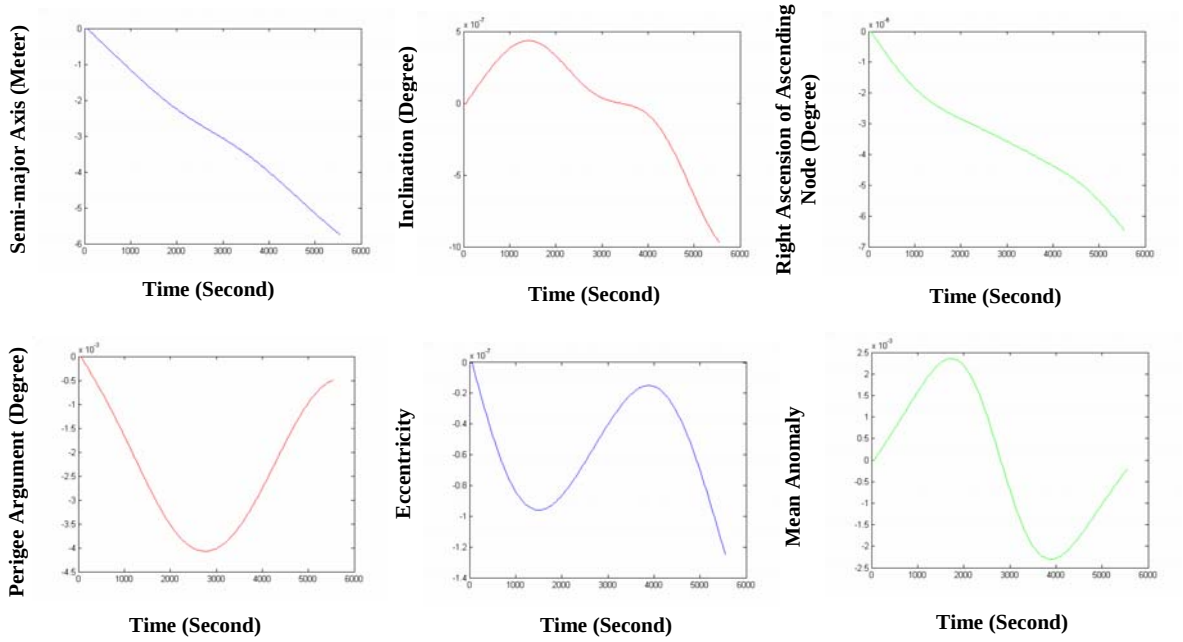


**Figure 9.** The perturbation due to the air drag in orbital elements in 1 revolution.

**Table 1.** Perturbing accelerations and orbital elements.

| | a | i | Ω | ω | e | M |
|---|---|---|---|---|---|---|
| Geopotential Acceleration | 20000 m, Periodic | $3.8^\circ \times 10^{-3}$ Periodic | $1.5^\circ$ Secular | $10^\circ$ Complex | 0.0004 Complex | $15^\circ$ Periodic |
| Solid Tide | 0.5 m Periodic | $5.5^\circ \times 10^{-4}$ Periodic | $3^\circ$ Periodic | $1.1^\circ \times 10^{-3}$ Periodic | $4 \times 10^{-7}$ m Secular | $1.1^\circ \times 10^{-3}$ Complex |
| Third body | 0.8 m Periodic | $3^\circ \times 10^{-5}$ Secular | $1.1^\circ \times 10^{-5}$ Secular | $2.5^\circ \times 10^{-3}$ Periodic | $2.5^\circ \times 10^{-7}$ Periodic | $2.5^\circ \times 10^{-3}$ Complex |
| General relativity | 0.08 m Periodic | $7^\circ \times 10^{-8}$ Periodic | $4^\circ \times 10^{-8}$ Periodic | $1.2^\circ \times 10^{-4}$ Complex | $2^\circ \times 10^{-9}$ Periodic | $12^\circ \times 10^{-5}$ Periodic |
| Ocean tide | 0.2 m Periodic | $2.5^\circ \times 10^{-7}$ Periodic | $6^\circ \times 10^{-7}$ Secular | $2^\circ \times 10^{-4}$ Periodic | $7^\circ \times 10^{-8}$ Secular | $2^\circ \times 10^{-4}$ Periodic |
| Rotational deformation | 3.5 m Periodic | $2^\circ \times 10^{-5}$ Periodic | $1.6^\circ \times 10^{-4}$ Secular | $3.5^\circ \times 10^{-3}$ Periodic | $5^\circ \times 10^{-7}$ Periodic | $4^\circ \times 10^{-3}$ Complex |
| Solar radiation | 2 m Periodic | $1.2^\circ \times 10^{-5}$ Periodic | $6^\circ \times 10^{-4}$ Periodic | $2.5^\circ \times 10^{-3}$ Secular | $1.2^\circ \times 10^{-6}$ Secular | $12^\circ \times 10^{-4}$ Periodic |
| Air drag | 6 m Secular | $5^\circ \times 10^{-7}$ Complex | $7^\circ \times 10^{-6}$ Secular | $4.5^\circ \times 10^{-3}$ Periodic | $1.4^\circ \times 10^{-7}$ Periodic | $2.5^\circ \times 10^{-3}$ Periodic |

The Table 1 shows the maximum values of the perturbations in orbital elements due to each one of the disruptive accelerations. The word complex means a combination of secular and periodic variations. As one can see from the table, the geopotential acceleration has the largest effect. The semi major axis of the orbital ellipse has periodic variations under almost all of the perturbing accelerations except the air drag. The inclination's behavior is secular for the third body effect, and for the rest of the acceleration it is periodic. The right ascension of the ascending

node acts periodically for solid tide, general relativity, and solar radiation, but it acts as secular for the rest of the accelerations. Perigee argument has just secular variation due to the solar radiation. The eccentricity behaves periodically for geopotential, the third body, general relativity, rotational deformation, and air drag. The mean anomaly usually varies periodically but it is secular for some disturbing forces.

## 6 CONCLUSIONS AND RECOMMENDATIONS

In this paper the perturbing accelerations acting on a low Earth orbiting satellite were investigated using the second-order vector differential equations of motion of a satellite. The output of numerical integration process is the position and velocity vector of the satellite. The perturbations were calculated and presented on either a satellite-centered coordinate system or on the orbital elements. According to the numerical studies one can see that the geopotential accelerations affect the semi major axis of CHAMP satellite in about 20000 m, which is much larger in comparison with other satellites. As an example, this value is about 2000 for GPS satellites in one revolution. The behaviors of the perturbations are the same with other satellites but their magnitudes are different. As one can see in table 1, the geopotential acceleration has the largest effect. The semi major axis of the orbital ellipse has periodic treatment for all perturbing acceleration except the air drag. The inclination's behaviour is secular under the third body effect, but periodic under the rest of the accelerations. The right ascension of the ascending node acts periodically for solid tide, general relativity, and solar radiation, but it acts as secular for the rest of the accelerations. Perigee argument has just secular variation due to the solar radiation. The eccentricity acts periodically for geopotential, third body, general relativity, rotational deformation, and air drag. The mean anomaly usually varies periodically but it is secular for some disturbing forces. The effects of the general relativity and the ocean tide are small. Their numerical values are contaminated with computation noises. In such cases, it is recommended to use a more accurate integration method for precise applications. Usually the Störmer-Cowel predictor-corrector algorithm of 11-order is used for this purpose. For computing more precise orbit the integrated orbit should be constrained with GPS observations of satellite positions. Usually the Kalman filter scheme is better to use in which the transition matrix of the filter is evaluated using linearized equations of motion. But using the numerical integration method as a predictor is suggested and the corrector is based on GPS observations. Also, one can test the accuracy of the orbit integration scheme by analyzing the variance. In terms of magnitude, the perturbations of a low orbiting satellite can be arranged as the geopotential perturbation, air drag, rotational deformation, third body effect, solid Earth tide, ocean tide, and the general relativity.

## REFERENCES

Babolian, E., and Malek Nejad, K., 1994, Numerical computations, University of Elm va San'at publication, Tehran, Iran.

Buffet, A., 1985, Short arc orbit improvement of GPS satellite, MSc thesis, University of Calgary, Department of Geodesy and Geomatics Engineering, Calgary, Canada.

Eanes, R. J., and Bettadpur, S., 1995, The CSR 3.0 Global Ocean tide model diurnal and semi diurnal Ocean Tides from TOPEX/Poseidon Altimetry, Technical Report, University of Texas, United States of America.

Eshagh, M., 2003a, Consideration of behaviour of orbital elements with respect to different degree and order of geopotential Models, submitted to J. Earth Space Phys. Geophysics Institute, University of Tehran, Tehran, Iran.

Eshagh, M., 2003b, Comparison of different numerical integration methods of orbit integration, submitted to J. Earth Space Phys. Geophysics Institute, University of Tehran, Tehran, Iran.

Eshagh, M., 2003c, Consideration of the effect of Gravitational and non-gravitational forces acting on a low Earth orbiting satellite, paper to be presented in 11-th National Iranian Geophysical Conference, 1-3 December, National Geological Center, Tehran, Iran.

Eshagh, M., 2005, Step variable numerical orbit integration of a low Earth orbiting satellite, J. Earth Space Phys. Geophysics Institute, University of Tehran, Tehran, Iran, **31**, 1-12.

Eshagh, M., and Najafi Alamdari M., 2003, Precise orbit determination of a low Earth orbiting satellite, MSc thesis, K. N. Toosi University of Technology, Tehran, Iran.

Eshagh, M., and Najafi Alamdari, M., 2005a, Investigation of orbital perturbations of a low Earth orbiting (LEO) satellite, paper to be presented in NATM June 27-29, Institute of Navigation ION 61 St. Cambridge,

Massachusetts, United States of America.

Eshagh, M., and Najafi Alamdari, M., 2005b, Numerical orbit integration of a low Earth orbiting satellite, paper to be presented in European navigation conference, GNSS 2005, German Institute of Navigation, Munchen, Germany.

Eshagh, M., and Najafi Alamdari, M., 2005c, Numerical integration and orbital perturbation of CHAMP satellite's orbit, paper to be presented in GNSS 2005, January, Institute of Navigation, San Diego, California United States of America.

Hofmann, W., and Lichtenegger, H., and Collins, J., 2001, Global positioning system, theory and practice, revised edition, Springer Wienna New York.

Leick, A., 1995, GPS satellite surveying, 2nd edn. Wiley interscience, New York Chichester Toronto Brisbane Singapore.

McCarthy. D., 1996, IERS Technical Note 21., US Naval Observatory, Central Bureau of IERS-Observatoire, Paris 61, avenue de l'Observatoire, France.

Parrot, D., 1989, Short arc orbit improvement for GPS satellites, MSc thesis, Department of Surveying Engineering, University of New Brunswick, Canada.

Rim, H. J., and Schutz, B. E., 2001, Precision orbit determination (POD), Geoscience laser and altimeter satellite system, University of Texas, United States of America.

Santos, M. C., 1994, On real time orbit improvement for GPS satellites, Ph.D thesis, Department of Geodesy and Geomatics Engineering, University of New Brunswick, Canada.

Seeber, G., 2003, Satellite Geodesy, 2nd completely revised and extended edition, Walter de Gruyter. Berlin. New York.

Su. H., 2000, Orbit determination of IGSO, GEO and MEO satellites, Ph.D thesis, Department of Geodesy, University of Bundeswehr, Munchen, Germany

Wolf. R., 2000, Satellite orbit and ephemeris determination using inter satellite links, Ph.D thesis, Department of Geodesy, University of Bundeswehr, Munchen, Germany.